Journal of the Serbian Chemical Society
JSCS-info@shd.org.rs • www.shd.org.rs/JSCS

ACCEPTED MANUSCRIPT

Journal of the Serbian Chemical Society
JSCS-info@shd.org.rs • www.shd.org.rs/JSCS
*J. Serb. Chem. Soc.***00(0)** 1-14 (2024)
JSCS–13072
Original scientific paper
Published DD MM, 2024

Different electrode modification protocols for evaluating the water-splitting properties of a P(V)-metalloporphyrin

BOGDAN-OVIDIU TARANU*

National Institute of Research and Development for Electrochemistry and Condensed Matter, Dr. A. Paunescu Podeanu Street, No. 144, 300569 Timisoara, Romania.

(Received 4 October; revised 25 November; accepted 16 December 2024)

Abstract: Water electrolysis is currently a notable research domain, having the identification of highly active, stable, and low-cost electrocatalysts as one of its most important pursuits. Herein, an A_4 P(V)-centered metalloporphyrin – (5,10,15,20-tetraphenylporphinato) dichlorophosphorus (V) chloride – was evaluated in terms of its electrocatalytic water-splitting activity in acidic, neutral, and alkaline media. The experiments were performed on electrodes modified with the porphyrin complex using different protocols, and the most electrocatalytically active sample was the one obtained by applying a catalyst ink containing the metalloporphyrin and Carbon Black on glassy carbon. The best results were observed for the strongly alkaline medium (1 mol L^{-1} KOH), in which the electrode exhibited a hydrogen evolution reaction overpotential of 0.77 V and a Tafel slope of 0.135 V dec^{-1}. Its stability was outlined by chronoamperometry and Raman spectroscopy. The results supplement the available data regarding the properties and applicative potential of metalloporphyrins and outline the implications of using different electrode manufacturing procedures.

Keywords: electrocatalyst; aggregate; hydrogen evolution reaction; oxygen evolution reaction; macrocycle.

INTRODUCTION

The ongoing struggles to replace fossil energy sources with renewable ones, to manage the increasing energy demand, the expanding global economy and the fast-growing population have led researchers to consider hydrogen as the auspicious energy carrier of the future.[1] Because the energy infrastructure is currently reliant to a great extent on finite and non-renewable energy sources a global energy crisis can only be delayed but not avoided. Furthermore, it is known that the use of fossil fuels has a detrimental effect on the environment.[2] The problems surrounding them have led to a concerted effort by researchers to study

* Corresponding author. E-mail: b.taranu84@gmail.com; Phone: +40740955505
https://doi.org/10.2298/JSC241004105T

the potential of alternative energy sources and to find a suitable energy carrier.[3] The scientific literature outlines hydrogen as an environmentally friendly energy carrier with highly desirable properties.[4] Hydrogen can be generated *via* several methods but only some of them are non-polluting in the sense that they rely on renewable energy sources (water, biomass, wind power, and solar power).[5] Since the goal is to obtain hydrogen in ways that avoid further environmental pollution the focus is on the eco-friendly approaches. Water-splitting, a method for hydrogen generation *via* the direct decomposition of water into its elements is considered by researchers to be the most promising way for replacing the fossil fuel-based energy infrastructure.[6] During water electrolysis pure hydrogen and oxygen are obtained from the splitting of water molecules using electric current.[7] Electrocatalysts play an essential role since they decrease the kinetic energy barrier between the two half-cell reactions – the hydrogen and the oxygen evolution reactions (HER and OER) – involved in the process.[8] Currently, the benchmark electrocatalysts are based on noble metals that cannot be used for large-scale hydrogen production because they are costly and scarce.[9] Many alternatives have been proposed that are cheaper, less scarce or even abundant, and exhibit fairly high catalytic efficiency and stability.[10] However, none of them have replaced the noble metal-based electrocatalysts.

Porphyrins are a class of aromatic compounds that have been shown to exhibit water-splitting catalytic activity.[11-13] They share a common feature known as the porphyrin macrocycle, they can be substituted peripherally with a wide variety of functional groups, and the center of the macrocycle can be metalated with almost every known metal ion – leading to the formation of metalloporphyrins. Changes to the chemical structure of porphyrins result in changes to their properties which can turn them into candidates for different types of applications. Furthermore, single molecules can associate with neighboring ones to form stable and well-defined aggregates with features that are often different from those of their constituents.[14,15]

The electrocatalytic water-splitting properties of metalloporphyrins have been investigated at least since 1985.[16] Recent publications indicate the persistent interest in the applicative potential of metalated porphyrin derivatives for the water-splitting field.[11,17]

This paper presents the study of the water-splitting properties of a symmetrically substituted A_4 P(V)-centered metalloporphyrin, namely (5,10,15,20-tetraphenylporphinato) dichlorophosphorus (V) chloride, in solutions covering a wide pH range. Identified publications involving this metalated porphyrin do not contain investigations of its HER and OER electrocatalytic properties.[18-22] The experimental results obtained during the testing of electrodes modified with the porphyrin complex by employing different protocols supplement the currently available data regarding the characteristics and

applicative potential of metalloporphyrins and outline the consequences of using diverse procedures to manufacture electrodes.

EXPERIMENTAL

Materials and reagents

The porphyrin complex - (5,10,15,20-tetraphenylporphinato) dichlorophosphorus (V) chloride - was purchased from Porphyrin Systems (Halstenbek, Germany) and used as received. The chemical structure of the porphyrin complex is shown in Scheme 1.

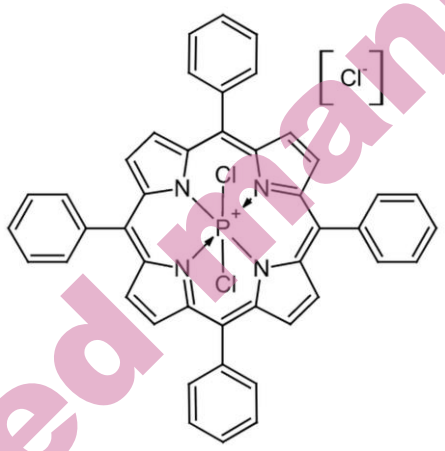

Scheme 1. The chemical structure of (5,10,15,20-tetraphenylporphinato) dichlorophosphorus (V) chloride.

Dichloromethane (DCM), tetrahydrofuran (THF), acetonitrile (CH_3CN), N,N-dimethylformamide (DMF) and Nafion® 117 solution were acquired from Sigma Aldrich (Saint Louis, MO, USA). Ethanol 99.5 % (EtOH) and acetone were obtained from Honeywell (Charlotte, NC, USA) and Chimreactiv (Bucharest, Romania). Benzonitrile (PhCN), dimethylsulfoxide (DMSO), KOH, KCl and H_2SO_4 98 % were purchased from Merck (Darmstadt, Germany). All reagents were used as procured. GC (glassy carbon) tablets were received from Andreescu Labor & Soft SRL (Bucharest, Romania) and Carbon Black - Vulcan XC 72 from Fuell Cell Store (Bryan, TX, USA). Double-distilled water was used to prepare all aqueous solutions.

Electrode modification protocols

The first protocol employed to manufacture the metalloporphyrin-based electrodes consists of the drop-casting on the surface of GC tablets of solutions obtained by dissolving the porphyrin complex in organic solvents having different polarity values. Solvent polarity decreases in the following order: DMSO > DMF > CH_3CN > PhCN > EtOH > THF > DCM.[23,24] The drop-casted volume was 10 µL and the drying of the covered GC substrates was performed at 40 °C. The resulting electrodes were modified with one metalloporphyrin layer. Samples with two and three layers were also prepared by repeating the mentioned procedure. Table I presents the codes used to identify the electrodes.

TABLE I. The codes for identifying the electrodes modified utilizing the first protocol

Electrode codes	Solvents	Porphyrin layers	Electrode codes	Solvents	Porphyrin layers
$GC_{P1\text{-}DMSO\text{-}1}$		1	$GC_{P1\text{-}EtOH\text{-}1}$		1
$GC_{P1\text{-}DMSO\text{-}2}$	DMSO	2	$GC_{P1\text{-}EtOH\text{-}2}$	EtOH	2
$GC_{P1\text{-}DMSO\text{-}3}$		3	$GC_{P1\text{-}EtOH\text{-}3}$		3
$GC_{P1\text{-}DMF\text{-}1}$		1	$GC_{P1\text{-}THF\text{-}1}$		1
$GC_{P1\text{-}DMF\text{-}2}$	DMF	2	$GC_{P1\text{-}THF\text{-}2}$	THF	2
$GC_{P1\text{-}DMF\text{-}3}$		3	$GC_{P1\text{-}THF\text{-}3}$		3
$GC_{P1\text{-}CH3CN\text{-}1}$		1	$GC_{P1\text{-}DCM\text{-}1}$		1
$GC_{P1\text{-}CH3CN\text{-}2}$	CH_3CN	2	$GC_{P1\text{-}DCM\text{-}2}$	DCM	2
$GC_{P1\text{-}CH3CN\text{-}3}$		3	$GC_{P1\text{-}DCM\text{-}3}$		3
$GC_{P1\text{-}PhCN\text{-}1}$		1			
$GC_{P1\text{-}PhCN\text{-}2}$	PhCN	2			
$GC_{P1\text{-}PhCN\text{-}3}$		3			

Electrode manufacturing was also performed by following a different protocol, based on a previously reported study.[25] Catalyst inks containing the porphyrin complex as such or mixed with Carbon Black resulted after a 30-minute ultrasonication treatment. The surface of the GC tablets was covered by drop-casting a catalyst ink volume of 10 µL. This stage was followed by the drying of the modified substrates at 40 °C which led to the obtaining of the modified electrodes. Table II shows the codes for identifying the samples and the ink compositions.

TABLE II. The codes for identifying the electrodes modified utilizing the second protocol

Electrode codes	Porphyrin amount (mg)	Carbon black (mg)	Nafion solution (µL)	Double-distilled water (µL)
GC_{P1}	10	-	50	450
$GC_{P1\text{-}CB}$	5	5	50	450

Electrochemical study

Three electrodes were connected to a Voltalab potentiostat model PGZ 402 from Radiometer Analytical (Lyon, France) and were subsequently inserted into a glass cell. One of the electrodes – a Pt plate with a geometric surface (S_{geom}) of 0.8 cm^2 – was used as the counter electrode. The reference electrode was the Ag/AgCl (sat. KCl) electrode. Each metalloporphyrin-modified electrode served as the working electrode. It was placed inside a polyamide support that ensured a constant S_{geom} of 0.28 cm^2. Acidic (0.1 mol L^{-1} H_2SO_4), neutral (0.1 mol L^{-1} KCl) and strongly alkaline (1 mol L^{-1} KOH) electrolyte solutions were prepared in order to cover a wide pH range. Before each HER experiment the electrolyte solutions were thoroughly deaerated with high-purity nitrogen. The OER and HER linear sweep voltammograms (LSVs) were *IR*-corrected and recorded at a scan rate (v) of 5 mV/s.[26] Unless stated otherwise, the electrochemical parameters j and E are the geometric current density and the electrochemical potential expressed *vs.* the Reversible Hydrogen Electrode (RHE). The E values were represented in terms of the RHE with Equation (S-1) – see the Supplementary Material. Equations (S-2) and (S-3) were used to calculate the O_2 and H_2 evolution overpotentials (η_{OER} and η_{HER}), while Equation (S-4) is the Tafel equation.[27-29]

Analysis by SEM and Raman spectroscopy

SEM analysis was carried out with a tabletop scanning electron microscope, CUBE II model, from EmCrafts Co. Ltd. (Kwangju, South Korea). A MultiView-2000 system from Nanonics Imaging Ltd. (Jerusalem, Israel) equipped with a Shamrock 500i spectrograph from Andor (Essex, UK) was used to record the Raman spectra.

RESULTS AND DISCUSSION

Tests on the electrodes manufactured using the first protocol

The LSVs recorded in 0.1 mol L^{-1} H_2SO_4 solution during the OER tests performed on electrodes obtained with the first modification protocol evidence their low electrocatalytic activity, characterized by high overpotentials and low current densities (Fig. S-1 from the Supplementary Material). Fig. S-1a, Fig. S-1b and Fig. S-1c present the results obtained for the electrodes modified with one, two and three metalloporphyrin layers. Relative to the unmodified GC sample (GC_0) only $GC_{P1\text{-}DMF\text{-}1}$ and $GC_{P1\text{-}EtOH\text{-}1}$ exhibit a slightly higher activity. In the neutral electrolyte solution (Fig. S-2) several of the modified electrodes display higher OER activity compared with GC_0, but under these mild conditions the overpotentials are high and the current densities low. The anodic LSVs recorded in the strong alkaline solution can be seen in Fig. S-3. The lowest η_{OER} values were determined for $GC_{P1\text{-}DMSO\text{-}1}$ (Fig. S-3a). At j = 10 mA cm^{-2}, a benchmark value at which the overpotential is often specified, η_{OER} = 1.15 V.[30]

The cathodic polarization curves obtained during the HER experiments performed on the electrodes modified with the first protocol in the acidic, neutral, and alkaline media are shown in Fig. S-4, Fig. S-5 and Fig. 1. The lowest η_{HER} value in 0.1 mol L^{-1} H_2SO_4 solution belongs to $GC_{P1\text{-}EtOH\text{-}3}$ (1.54 V at j = –10 mA cm^{-2}) – Fig. S-4c. In 0.1 mol L^{-1} KCl solution $GC_{P1\text{-}CH3CN\text{-}1}$ (Fig. S-5a) and $GC_{P1\text{-}DMF\text{-}2}$ (Fig. S-5b) have the lowest η_{HER} value at j = –10 mA cm^{-2}, of ~ 1.38 V. The best results are observed in the strongly alkaline medium for the electrodes modified with the porphyrin complex drop-casted from DMF in one layer (Fig. 1a) and from DMSO in one (Fig. 1a), two (Fig. 1b) and three layers (Fig. 1c). A η_{HER} value of ~ 0.90 V was determined in all these cases and it reveals the limits of the modification protocol used to manufacture the tested electrodes.

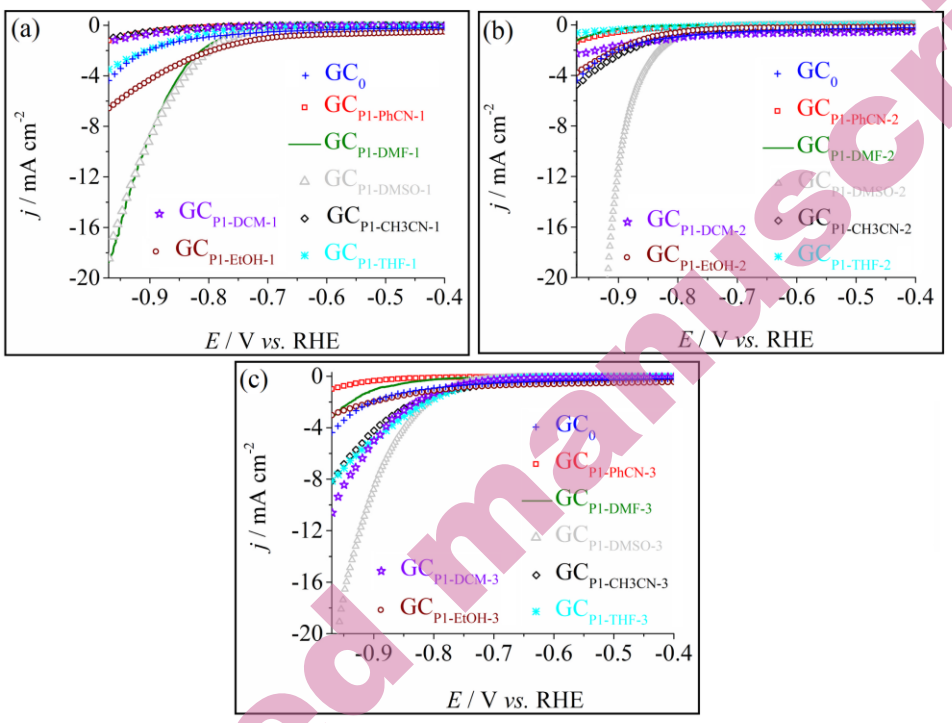

Fig. 1. Cathodic polarization curves recorded on GC_0 and on (a) $GC_{P1\text{-}PhCN\text{-}1}$, $GC_{P1\text{-}DMF\text{-}1}$, $GC_{P1\text{-}DMSO\text{-}1}$, $GC_{P1\text{-}CH3CN\text{-}1}$, $GC_{P1\text{-}THF\text{-}1}$, $GC_{P1\text{-}DCM\text{-}1}$, $GC_{P1\text{-}EtOH\text{-}1}$; (b) $GC_{P1\text{-}PhCN\text{-}1}$, $GC_{P1\text{-}DMF\text{-}1}$, $GC_{P1\text{-}DMSO\text{-}1}$, $GC_{P1\text{-}CH3CN\text{-}1}$, $GC_{P1\text{-}THF\text{-}1}$, $GC_{P1\text{-}DCM\text{-}1}$, $GC_{P1\text{-}EtOH\text{-}1}$ and (c) $GC_{P1\text{-}PhCN\text{-}1}$, $GC_{P1\text{-}DMF\text{-}1}$, $GC_{P1\text{-}DMSO\text{-}1}$, $GC_{P1\text{-}CH3CN\text{-}1}$, $GC_{P1\text{-}THF\text{-}1}$, $GC_{P1\text{-}DCM\text{-}1}$, $GC_{P1\text{-}EtOH\text{-}1}$. Electrolyte solution: 1 mol L^{-1} KOH. v = 5 mV s^{-1}.

It was pointed out in the Introduction section that porphyrin molecules can self-assemble into aggregates. To see if this is also the case with the studied porphyrin complex, a modified electrode, $GC_{P1\text{-}DMSO\text{-}1}$, was selected for SEM characterization. The micrographs recorded in two different areas on the surface of the sample are rendered in Fig. 2. Both images (Fig. 2a and Fig. 2b) show that the metalloporphyrin molecules associated as irregular aggregates with dimensions in the micrometric domain. These structures are sporadic and their distribution is inhomogeneous. It is known that inhomogeneities act as active site generators during electrocatalytic processes.[28]

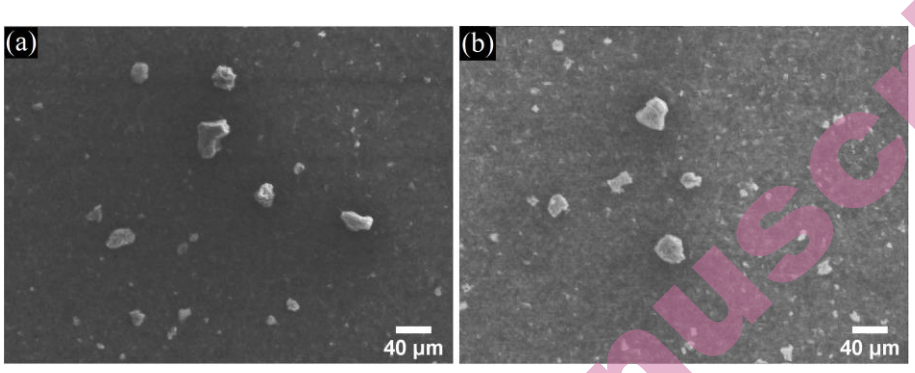

Fig. 2. SEM images recorded in two different areas on the surface of the $GC_{P1\text{-}DMSO\text{-}1}$ electrode. (a) The micrograph obtained for the first area selected for analysis. (b) The micrograph obtained for the second area selected for analysis.

Tests on the electrodes manufactured using the second protocol

The anodic LSVs recorded on the metalloporphyrin-modified electrodes manufactured using the second protocol described in the Experimental section are shown in Fig. S-6. In the acidic environment (Fig. S-6a) $GC_{P1\text{-}CB}$ and GC_{P1} display low OER activity and features corresponding to oxidation processes are present on the polarization curves. In the neutral and strongly alkaline solutions (Fig. S-6b and S-6c) the η_{OER} values determined for GC_{CB} are lower than for the other electrodes, indicating that the presence of the porphyrin derivative negatively affects the OER activity of the metalloporphyrin-modified electrodes.

Fig. 3 shows the cathodic LSVs obtained during the HER experiments. In the 0.1 mol L^{-1} H_2SO_4 and 0.1 mol L^{-1} KCl solutions the highest electrocatalytic activity is displayed by GC_{CB} (Fig. 3a and Fig. 3b), but in the strongly alkaline medium the lowest overpotential values belong to GC_{P1} and $GC_{P1\text{-}CB}$ (Fig. 3c). The η_{HER} value determined for $GC_{P1\text{-}CB}$ at $j = -10$ mA cm^{-2} is 0.77 V and it outlines this electrode as having the highest HER electrocatalytic activity.

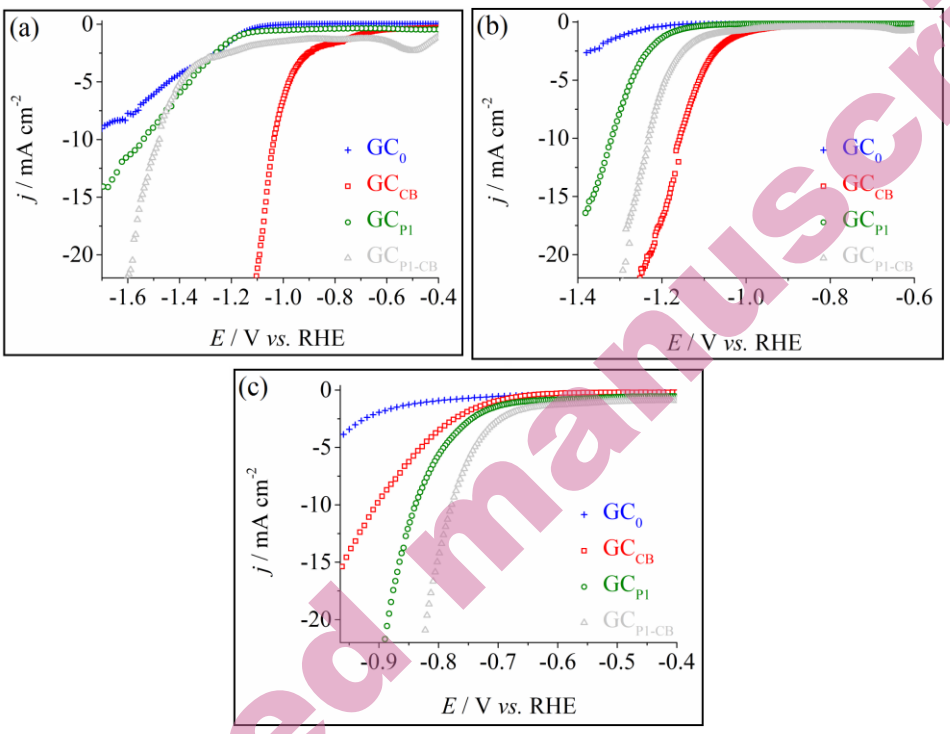

Fig. 2. Cathodic polarization curves recorded on GC_0, GC_{CB}, GC_{P1} and $GC_{P1\text{-}CB}$ in the following electrolyte solutions: (a) 0.1 mol L^{-1} H_2SO_4, (b) 0.1 mol L^{-1} KCl and (c) 1 mol L^{-1} KOH. v = 5 mV s^{-1}.

The electrochemical properties of $GC_{P1\text{-}CB}$ were further evaluated and the results are presented in Fig. 4. Fig. 4a shows the plot of the capacitive current density (j_{dl}) *vs.* the scan rate for the specified electrode, while the Tafel plot and the chronoamperogram recorded during its electrochemical stability testing are rendered in Fig. 4b and Fig. 4c.

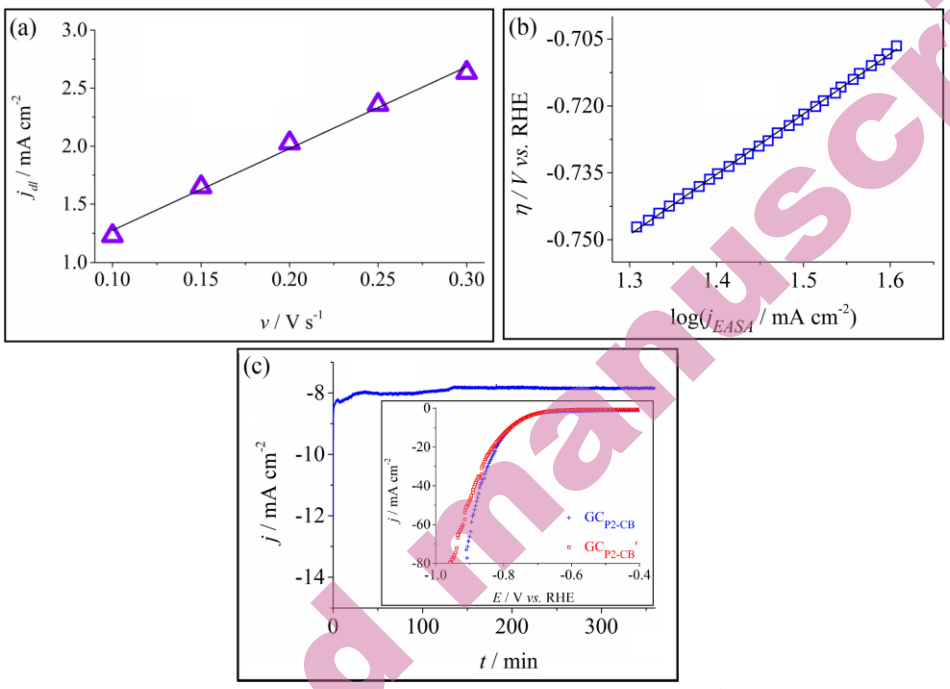

Fig. 3. (a) The j_{dl}-v graphical representation for GC_{P1-CB} in 0.1 mol L^{-1} KCl solution. (b) The Tafel plot for GC_{P1-CB} in 1 mol L^{-1} KOH solution. The current density (j_{EASA}) values from the plot are *EASA*-normalized. (c) Chronoamperogram obtained on GC_{P1-CB} in 1 mol L^{-1} KOH solution and inset with the LSVs obtained on the same electrode before (GC_{P1-CB}) and after (GC_{P1-CB}') the electrochemical stability test (1 mol L^{-1} KOH solution, v = 5 mV s^{-1}).

The j_{dl} values required to represent the plot from Fig. 4a were obtained by carrying out cyclic voltammetry experiments in 0.1 mol L^{-1} KCl solution at v values of 10, 20, 30, 40 and 50 mV s^{-1} in an E range with no Faradic currents. The recorded data was subsequently used in equation (S-5) from the Supplementary Material.[31] The linear increase observed in Fig. 4a correlates with the charging and discharging of the Helmholtz double-layer.[32] The absolute value of the plot's slope is the electrode's electric double layer capacitance (C_{dl}) deriving from the stored charge in the double-layer at the electrode/electrolyte solution interface.[31] This parameter is important for the supercapacitors domain in which a higher value is preferred to a lower one.[33] Table III presents the C_{dl} value determined for GC_{P1-CB} together with the R^2, R_f (the roughness factor) and *EASA* (the electrochemically active surface area) values. The R_f value is equal to the ratio between the real surface of the electrode and S_{geom} and was calculated by dividing C_{dl} to 60 µF cm^{-2}, which is the specific capacitance of a smooth oxide surface.[34] The *EASA* was calculated with equation (S-6).[31]

TABLE III. The C_{dl}, R^2, R_f and *EASA* values obtained for the $GC_{P1\text{-}CB}$ electrode

Electrode	C_{dl} / mF cm^{-2}	R^2	R_f	*EASA* / cm^2
$GC_{P1\text{-}CB}$	7.05	0.9915	117.5	32.9

There are two reasons why the *EASA* was estimated. Firstly, it is known that the value of this parameter is directly proportional to the number of catalytically active centers participating in an electrocatalytic process, including in water-splitting.[35] Secondly, it was used to represent the Tafel plot from Fig. 4b which is required to determine the Tafel slope – a parameter relevant to an electrode's water-splitting activity, whose lower value indicates faster reaction kinetics.[15] The Tafel slope was found to be 0.135 V dec^{-1} (R^2 = 0.9993). The high pH value of the electrolyte solution leads to the covering of a high degree of the electrode's surface with H_2 bubbles. These in turn affect the value of the slope by making it higher than 0.12 V dec^{-1}.[36] A slope between 0.04 and 0.12 V dec^{-1} points to the HER occurring *via* a Volmer-Heyrovsky mechanism and to the rate of the discharge step being consistent with that of the desorption step.[37] However, under alkaline conditions when the value exceeds the upper limit of the specified interval a Volmer-limited mechanism is usually involved, with the Volmer step being faster than the Heyrovsky step.[36]

The electrochemical stability test performed on $GC_{P1\text{-}CB}$ lasted 6 h and the chronoamperogram obtained by maintaining a constant *E* value of 0.77 V *vs.* RHE is presented in Fig. 4c. It can be seen that the current density steadily evolves towards a constant value. At *t* = 135 min this value is ~ –7.8 mA cm^{-2}. The electrode is relatively stable throughout the experiment. The inset in Fig. 4c presents the LSVs recorded on the electrode before and after the test. The two curves overlap almost perfectly at the current density of –10 mA cm^{-2}. This result is a positive indication of the sample's stability which is further evidenced using Raman Spectroscopy. Fig. S-7 shows the Raman spectra recorded on $GC_{P1\text{-}CB}$ before and after the chronoamperometric experiment. The signals identified on the spectrum obtained before the test are also present on the one obtained afterward, indicating that the electrode did not undergo notable structural changes.

Discussion regarding the HER properties of $GC_{P1\text{-}CB}$

The P(V)-centered porphyrin-based electrode manufactured using the second protocol described in the Experimental section and denoted $GC_{P1\text{-}CB}$ was shown to possess the highest HER catalytic activity. As a metalloporphyrin, its catalytic center is probably situated in the center of the metalated macrocycle, namely at the M-N_4 site.[38,39] The *EASA* value obtained for the electrode is high compared to its geometric surface (*EASA* = 32.9 cm^2 and S_{geom} = 0.28 cm^2), which points to the presence of inhomogeneities and to the sample benefiting from a relatively large number of active sites. Charge transport effects also play an important role in the

electrocatalytic behavior of metalloporphyrins. Aside from the charge transport occurring between adjacent molecules through non-covalent π-π interactions, there is also the one taking place at the interface between the molecules and the GC support.[38] The P(V)-metalloporphyrin has a phosphorous metal atom located in the center of its macrocycle. This atom is hexacoordinated and the macrocycle possesses a distorted octahedral geometry. The P atom is less electronegative compared with the C atoms of the GC and induces an electronegative doping effect on the substrate's surface. The electron-donating and electron-withdrawing effects of the functional moieties that porphyrin derivatives are substituted with constitute another factor influencing their water-splitting properties. Electron-withdrawing substituents in particular decrease the macrocycle's electron density leading to a decrease in the HER overpotential.[39] The phenyl groups of the porphyrin complex exhibit only a weak electron-withdrawing inductive effect which in turn has a weak impact on the overpotential. The pH of the electrolyte solution should not be overlooked either since its significant effect on an electrode's water-splitting performance is well known.[40,41] As specified, the strongly alkaline environment in which $GC_{P1\text{-}CB}$ is immersed affects the value of the Tafel slope and is responsible for slower HER kinetics.

What can be concluded about the water-splitting activity of the $GC_{P1\text{-}CB}$ electrode is that even though a relatively large number of catalytically active sites are probably present on its surface, other factors – such as an electronegative doping effect, a weak electron-withdrawing effect and the effect of the electrolyte solution's pH – negatively affect this property causing the decrease of the specimen's HER catalytic performance. The latter observation is reason to think the electrode will probably not end up being used in large-scale applications. Table S-I from the Supplementary Material compares the HER activity of $GC_{P1\text{-}CB}$ with that of other electrodes modified with free-base or metalated porphyrin derivatives. Its Tafel slope value is lower than most of the values mentioned in the table. While this is an advantage, its η_{HER} value is among the highest. The result points to the limitations of the utilized electrode modification strategy. Drop-casting-based protocols are low-cost and simple, but for improved water-splitting properties more sophisticated approaches could be required.

CONCLUSION

The water-splitting electrocatalytic properties of a symmetrically substituted A_4 P(V)-metalated porphyrin were evaluated in acidic, neutral and strongly alkaline electrolyte solutions. Metalloporphyrin-based electrodes were obtained by employing different electrode modification protocols. The results show that the specimen with the highest electrocatalytic activity is the one manufactured by drop-casting a catalyst ink containing the P(V)-porphyrin and Carbon Black on GC substrate. In 1 mol L^{-1} electrolyte solution, it displays a HER overpotential of 0.77

V (at $j = -10$ mA cm^{-2}) and a Tafel slope of 0.135 V dec^{-1}. It is relatively stable in the strongly alkaline medium but the high value of the overpotential prevents it from being used for commercial applications. Manufacturing protocols that utilize substrate modification techniques more complex than the simple drop-casting method will be assessed in upcoming investigations.

SUPPLEMENTARY MATERIAL

Additional data are available electronically at the pages of journal website: https://www.shd-pub.org.rs/index.php/JSCS/article/view/13072, or from the corresponding author on request.

Acknowledgements: The author would like to thank Dr. Adina Cata and Dr. Florina Stefania Rus from the National Institute for Research and Development in Electrochemistry and Condensed Matter (Timisoara, Romania) for performing the SEM and Raman analyses.

И З В О Д

РАЗЛИЧИТИ ПРОТОКОЛИ МОДИФИКАЦИЈЕ ЕЛЕКТРОДЕ P(V)-МЕТАЛПОРФИРИНИМА ЗА ИСПИТИВАЊЕ АКТИВНОСТИ ЗА РАЗЛАГАЊЕ ВОДЕ

BOGDAN-OVIDIU TARANU

National Institute of Research and Development for Electrochemistry and Condensed Matter, Dr. A. Paunescu Podeanu Street, No. 144, 300569 Timisoara, Romania.

Електролиза воде је тренутно значајна област истраживања, при чему је један од најважнијих задатака идентификација високо активних, стабилних и јефтиних електрокатализатора. У овом раду је испитан A_4 P(V)-центрирани металопорфирин (5,10,15,20-тетрафенилпорфинато) дихлорофосфор (V)-хлорид, у смислу његове електрокаталитичке активности за разлагање воде у киселој, неутралној и алкалној средини. Експерименти су урађени на електродама које су модификоване порфиринским комплексом коришћењем различитих протокола, при чему се као електрокаталитички најактивнији показао узорак добијен наношењем суспензије металопорфирина и угља развијене површине на стакласти угљеник. Најбољи резултати су добијени у јако алкалном раствору (1 mol L^{-1} KOH), у којем је електрода показала пренапетост реакције издвајања водоника од 0,77 V и Тафелов нагиб од 0,135 V dek^{-1}. Стабилност ове електроде је утврђена хроноамперометријом и Рамановом спектроскопијом. Резултати приказани у раду представљају допринос постојећим подацима о својствима и могућој примени металопорфирина те указују на утицај протокола припреме електроде на добијене резултате.

(Примљено 4. октобра; ревидирано 25. новембра; прихваћено 16. децембра 2024.)

REFERENCES

1. M. E. Rehman, S. Rehman, *Energy Rep.* **8** (2022) 5430 (https://doi.org/10.1016/j.egyr.2022.03.179)
2. C. Gursan, V. de Gooyert, *Renew. Sust. Energ. Rev.* **138** (2021) 1 (https://doi.org/10.1016/j.rser.2020.110552)

3. S. Banerjee, S. Kaushik, R. S. Tomar, *Global Scenario of Biofuel Production: Past, Present and Future*, in: *Prospects of Renewable Bioprocessing in Future Energy Systems*, A. A. Rastegari, A. N. Yadav, A. Gupta, Eds., Springer International Publishing, New York, USA, 2019, p. 499 (https://doi.org/10.1007/978-3-030-14463-0_18)
4. M. Saeed, J. Prashant, *Int. J. Hydrogen Energ.* **52** (2023) 1537 (https://doi.org/10.1016/j.ijhydene.2023.08.352)
5. S. E. Hosseini, M. A. Wahid, M. M. Jamil, A. A. M. Azli, M. F. Misbah, *Int. J. Energ. Res.* **39** (2015) 1597 (https://doi.org/10.1002/er.3381)
6. M. Rafique, R. Mubashar, M. Irshad, S. S. A. Gillani, M. Bilal Tahir, N. R. Khalid, A. Yasmin, M. A. Shehzad, *J. Inorg. Organomet. P.* **30** (2020) 3837 (https://doi.org/10.1007/s10904-020-01611-9)
7. X. Shi, X. Liao, Y. Li, *Renew. Energ.* **154** (2020) 786 (https://doi.org/10.1016/j.renene.2020.03.026)
8. W. Li, Y. Liu, A. Azam, Y. Liu, J. Yang, D. Wang, C. C. Sorrell, C. Zhao, S. Li, *Adv. Mater.* **Early View** (2024) 1 (https://doi.org/10.1002/adma.202404658)
9. N. Lv, Q. Li, H. Zhu, S. Mu, X. Luo, X. Ren, X. Liu, S. Li, C. Cheng, T. Ma, *Adv. Sci.* **10** (2023) 2206239 (https://doi.org/10.1002/advs.202206239)
10. A. Raveendran, M. Chandran, R. Dhanusuraman, *RSC Adv.* **13** (2023) 3843 (https://doi.org/10.1039/D2RA07642J)
11. O. V. Kharissova, Y. P. Mendez, B. I. Kharisov, A. L. Nikolaev, E. Luevano-Hipolito, L. T. Gonzalez, *Particuology* **90** (2024) 236 (https://doi.org/10.1016/j.partic.2023.12.008)
12. Q. Li, Y. Bao, F. Bai, *MRS Bull.* **45** (2020) 569 (https://doi.org/10.1557/mrs.2020.168)
13. B. Yao, Y. He, S. Wang, H. Sun, X. Liu, *Int. J. Mol. Sci.* **23** (2022) 6036 (https://doi.org/10.3390/ijms23116036)
14. M. Birdeanu, E. Fagadar-Cosma, *The Self-Assembly of Porphyrin Derivatives into 2D and 3D Architectures*, in *Quantum Nanosystems: Structure, Properties, and Interactions*, M. V. Putz, Ed., Apple Academic Press, Toronto, Canada, 2014, p. 173 (https://doi.org/10.1201/b17412)
15. B.-O. Taranu, E. Fagadar-Cosma, P. Sfirloaga, M. Poienar, *Energies* **16** (2023) 1212 (https://doi.org/10.3390/en16031212)
16. R. M. Kellett, T. G. Spiro, *Inorg. Chem.* **24** (1985) 2373 (https://doi.org/10.1021/ic00209a011).
17. I. Fratilescu, A. Lascu, B. O. Taranu, C. Epuran, M. Birdeanu, A.-M. Macsim, E. Tanasa, E. Vasile, E. Fagadar-Cosma, *Nanomaterials-Basel* **12** (2022) 1930 (https://doi.org/10.3390/nano12111930)
18. L. Salageanu, D. Muntean, H. F. George, A. Lascu, D. Anghel, I. C. Bagiu, E. Fagadar-Cosma, *Rev. Romana Med. Lab.* **28** (2020) 205 (https://doi.org/10.2478/rrlm-2020-0014)
19. E. Fagadar-Cosma, V. Badea, G. Fagadar-Cosma, A. Palade, A. Lascu, I. Fringu, M. Birdeanu, *Molecules* **22** (2017) 1787 (https://doi.org/10.3390/molecules22101787)
20. I. Creanga, A. Palade, A. Lascu, M. Birdeanu, I. Popa, *Fluorescent Sensor for Pb^{2+} Detection Based on Distorted Phosphorus (V) Porphyrin Ionic Complex*, in *Proceeding of the 20th International Symposium on Analytical and Environmental Problems*, (2014), University of Szeged, Hungary, *Proceedings of the 20th*

International Symposium on Analytical and Environmental Problems, University of Szeged, Szeged, 2014, p. 205 (ISBN 978-963-12-1161-0)
21. C. A. Marrese, C. J. Carrano, *Inorg. Chem.* **22** (1983) 1858 (https://doi.org/10.1021/ic00155a007)
22. H. Sharghi, A. H. Nejad, *Phosphorus Sulfur* **179** (2004) 2297 (https://doi.org/10.1080/10426500490484995)
23. L. R. Snyder, J. J. Kirkland, J. L. Glajch, *Practical HPLC Method Development*, John Wiley & Sons, New Jersey, USA, 1997 (https://doi.org/10.1002/9781118592014)
24. Z. Szabadai, L. Sbarcea, L. Udrescu, *Analiza fizică și chimică a medicamentului,* Victor Babes publishing house, Timisoara, Romania, 2016 (ISBN 978-606-786-020-7)
25. J. Chang, Q. Lv, G. Li, J. Ge, C. Liu, W. Xing, *Appl. Catal. B-Environ.* **204** (2017) 486 (https://doi.org/10.1016/j.apcatb.2016.11.050)
26. Y. Ge, Z. Lyu, M. Marcos-Hernandez, D. Villagran, *Chem. Sci.* **13** (2022) 8597 (https://doi.org/10.1039/D2SC01250B)
27. B.-O. Taranu, E. Fagadar-Cosma, *Processes* **10** (2022) 611 (https://doi.org/10.3390/pr10030611)
28. B.-O. Taranu, E. Fagadar-Cosma, *Nanomaterials-Basel* **12** (2022) 3788 (https://doi.org/10.3390/nano12213788)
29. B.-O. Taranu, S. F. Rus, E. Fagadar-Cosma, *Coatings* **14** (2024) 1048 (https://doi.org/10.3390/coatings14081048)
30. M. Poienar, B.-O. Taranu, P. Svera, P. Sfirloaga, P. Vlazan, *J. Therm. Anal. Calorim.* **147** (2022) 11839 (https://doi.org/10.1007/s10973-022-11435-z)
31. B. O. Taranu, S. D. Novaconi, M. Ivanovici, J. N. Goncalves, F. S. Rus, *Appl. Sci.-Basel* **12** (2022) 229708 (https://doi.org/10.3390/app12136821)
32. M. Kolbach, S. Fiechter, R. van de Krol, P. Bogdanoff, *Catal. Today* **290** (2017) 2 (https://doi.org/10.1016/j.cattod.2017.03.030)
33. B. Yao, S. Chandrasekaran, J. Zhang, W. Xiao, F. Qian, C. Zhu, E. B. Duoss, C. M. Spadaccini, M. A. Worsley, Y. Li, *Joule* **3** (2019) 459 (https://doi.org/10.1016/j.joule.2018.09.020)
34. M. L. F. Ciriaco, M. I. Silva-Pereira, M. R. Nunes, F. M. Costa, *Port. Electrochim. Acta* **17** (1999) 149 (https://doi.org/10.4152/pea.199902149)
35. Z. Zhou, W. Q. Zaman, W. Sun, L. M. Cao, M. Tariq, J. Yang, *Chem. Commun.* **54** (2018) 4959 (https://doi.org/10.1039/c8cc02008f)
36. F. Bao, E. Kemppainen, I. Dorbandt, R. Bors, F. Xi, R. Schlatmann, R. van de Krol, S. Calnan, *ChemElectroChem* **8** (2021) 195 (https://doi.org/10.1002/celc.202001436)
37. Z. Y. Wu, B. C. Hu, P. Wu , H. W. Liang, Z. L. Yu, Y. Lin, Y. R. Zheng, Z. Li, S. H. Yu, *NPG Asia Mater.* **8** (2016) e288 (https://doi.org/10.1038/am.2016.87)
38. S. Seo, K. Lee, M. Min, Y. Cho, M. Kim, H. Lee, *Nanoscale* **9** (2017) 3969 (https://doi.org/10.1039/c6nr09428g)
39. W. Zhang, W. Lai, R. Cao, *Chem. Rev.* **117** (2017) 3717 (https://doi.org/10.1021/acs.chemrev.6b00299)
40. S. Wang, A. Lu, C. J. Zhong, *Nano Converg.* **8** (2021) 4 (https://doi.org/10.1186/s40580-021-00254-x)
41. M. Durovic, J. Hnat, K. Bouzek, *J. Power Sources* **493** (2021) 229708 (https://doi.org/10.1016/j.jpowsour.2021.229708).